complex the Fe d population remains close to 8 during the H atom migration. However, there is some rearrangement of charge among the d orbitals of the complex during migration. The population of the d_{z^2} orbital, which is on the Fe-H axis of the hydride, increases from 0.18 in the hydride to 0.76 in the formyl. This charge comes mostly from the $d_{x^2-y^2}$ orbital. Since the d orbitals have very little overlap with the ligand orbitals, the population changes are presumed not to be due to bonding interactions lowering orbital energies but rather to repulsive interactions. In this case migration of the H atom removes the repulsive interaction of the hydride along the z axis so that after migration the d_{z^2} orbital is relatively more favored and the carbon atoms in the xy plane gain electrons to increase the repulsion in the xy plane. In the Fe_{12} cluster the various individual d orbital populations change very little during the migration. The larger ligand distances for the Fe_{12} cluster would contribute to the repulsive interactions having less effect for the cluster than for the complex.

Another important difference between the Fe_{12} cluster and the mononuclear metal complex is that the ligands interact with a band of orbitals on the cluster rather than with just a few orbitals on the complex. Orbital levels for the adsorbed CO and H and their reaction complex are given in Figure 8. In the case of the complex it was shown[36] that the migration leads to the occupation of an unfavorable high-energy orbital. Much of the H atom interaction occurred in this orbital. The d orbitals of the complex did not serve as a reservoir for charge, so that the bonding needed to be accommodated within the limited available s and p orbitals of the single Fe atom and the CO ligands. In contrast, for the cluster the CO and H interact with the broad sp band of the Fe_{12} cluster as shown in Figure 8 where the H atom contributes electron population to a number of molecular orbitals of the cluster formyl and the activated complex. Within the large number of orbitals in this band the CO and H interactions and the migration are accommodated without major orbital shifts and the migration proceeds without a large activation energy. Again, the d band of the cluster does not serve as a charge reservoir, but rather charge transfer is accomplished via the metal sp band.

Conclusions

Calculations have been carried out with a semiempirical procedure to calculate PES's for H migration onto a carbonyl to give a formyl structure for a noncatalyzed, a homogeneously catalyzed, and a heterogeneously catalyzed reaction. These calculations are consistent with the classical statement that a catalyst operates by providing a path with a reduced activation energy. The often-suggested analogy between heterogeneous and homogeneous is supported within the framework of these calculations by similarities in the H migration for the model homogeneous and heterogeneous catalytic processes, but distinct differences are also found. An important difference between the heterogeneous and homogeneous process is that the large number of orbitals in the metal valence band permits many different bonding structures with similar energies whereas the mononuclear homogeneous complex has only a few orbitals, which limits it to only a few stable structures. While this permits heterogeneous surfaces to catalyze many reactions, it also results in less selectivity for heterogeneous processes than for homogeneous processes. Experimentally, this is evident in the large number of products produced in the heterogeneously catalyzed Fischer-Tropsch synthesis. The theoretical foundation for the similarities and differences between heterogeneous and homogeneous catalysis has been illustrated with specific numbers for a particular case.

Acknowledgment is made to the donors of the Petroleum Research Fund, administered by the American Chemical Society, for partial support of this research and to the University of Arkansas for a computing time grant.

Registry No. CO, 630-08-0; $(CO)_4FeH^-$, 18716-80-8; formaldehyde, 50-00-0.

Ab Initio Studies on Silicon Compounds. 2.† On the Gauche Structure of the Parent Polysilane

Hiroyuki Teramae* and Kyozaburo Takeda

Contribution from the NTT Basic Research Laboratories, Musashino, Tokyo 180, Japan.
Received May 31, 1988

Abstract: Ab initio crystal orbital calculations are performed on the electronic structures of the parent polysilane. We examine the anaiysis of the energy band structure and the rotational potential in terms of the trans-gauche conformational transitions. We have found that the trans conformer is the ground state of the polysilane. The *gauche*-polysilane (GP) is 0.15 kcal/mol per SiH_2 unit above the *trans*-polysilane (TP). TP has a smaller band gap, lower ionization potential and greater electron delocalization than GP. The effective mass of the hole at the valence band edge is ultimately greater in GP than in TP. All our calculated results suggest that the conservation of near trans conformation is important in the improvement of the semiconductor characteristics of polysilanes.

1. Introduction

Polysilane is a one-dimensional polymer whose backbone consists of only silicon-silicon single bonds. Results of experiments, such as doping with an electron acceptor, photoconduction, and photoluminescence, show that polysilanes are semiconductors.[1] Polysilane is a semiconductive chain with a σ-type skeleton, unlike typical organic semiconductors with π-type frameworks, such as polyacetylene, polypyrrole, polythiophene, and so on. Almost every chemist feels it curious that the σ-electron is so delocalized that it can conduct an electric current. The resonance integrals between two σ-orbitals, however, do not vanish, and a σ-conjugation is possible.[2] We have previously reported some electronic band structure calculations on polysilanes.[3] In the previous calculations, we have naturally assumed the all-trans conformation for polysilanes because the carbon analogue polyethylene is well-known

† Part 1 of this series: Teramae, H. *J. Am. Chem. Soc.* **1987**, *109*, 4140.

(1) See review article: West, R. *J. Organomet. Chem.* **1986**, *300*, 327.
(2) Dewar, M. J. S. *J. Am. Chem. Soc.* **1984**, *106*, 669.
(3) (a) Teramae, H.; Yamabe, T.; Imamura, A. *Theor. Chim. Acta* **1983**, *64*, 1. (b) Takeada, K.; Teramae, H.; Matsumoto, N. *J. Am. Chem. Soc.* **1986**, *108*, 8186.

0002-7863/89/1511-1281$01.50/0

Table I. Optimized Structure of *trans*-Polysilane and *all-trans*-Si_nH_{2n+2} Clusters (Values Given in Angstroms and Degrees)

compd	basis set	r_{Si-Si}	∠Si-Si-Si	r_{Si-H}	∠H-Si-H	energy per SiH_2[a]
polysilane	STO-3G	2.245	114.1	1.425	106.0	−286.792 55
polysilane[b]	DZ	2.382	112.4	1.485	107.8	−290.043 73
polysilane[c]	SSZ	2.453	114.5	1.523	105.5	
polysilane[c]	LP-31G	2.264	119.0	1.493	100.3	
trisilane[b,d]	STO-3G	2.245	113.9	1.423	107.6	
tetrasilane[b,d]	STO-3G	2.246	114.1	1.425	106.0	−286.792 40
pentasilane[b,d]	STO-3G	2.247	114.2	1.425	105.7	−286.792 43
trisilane[b,d]	DZ	2.386	111.7	1.486	108.3	
tetrasilane[b,d]	DZ	2.387	112.1	1.486	108.1	−290.043 76
pentasilane[b,d]	DZ	2.387	112.7	1.486	107.8	−290.043 74
trisilane[b,d]	3-21G	2.383	109.6	1.489	108.9	
tetrasilane[b,d]	3-21G	2.383	110.8	1.489	108.4	−288.558 37
pentasilane[b,d]	3-21G	2.383	112.1	1.490	109.1	−288.558 41
trisilane[b,d]	6-31G**	2.358	112.7	1.481	108.3	
tetrasilane[b,d]	6-31G**	2.361	112.8	1.481	107.4	−290.081 55
pentasilane[b,d]	6-31G**	2.359	113.2	1.481	107.0	−290.081 57

[a] Total energy per SiH_2 unit for polymers and $E[H(SiH_2)_nH] - E[H(SiH_2)_{n-1}H]$ for clusters. [b] Present work. [c] From ref 1a. [d] Values are taken from the central segment.

to have this conformation, and there were few experimental measurements concerning the structural features of polysilanes.

Recent experimental results on the thermochromic changes of UV-absorption spectra, however, suggest that the conformation of the polysilane chain may change with temperature.[4] For example, λ_{max} for poly(di-*n*-butylsilane) shifts reversibly to longer wavelengths as the temperature is lowered; λ_{max} changes from 313 nm (4.0 eV) to 374 nm (3.3 eV) near 40 °C. The amount of thermochromic changes reaches 0.7 eV. Moreover, molecular mechanics (MM) calculations suggest that the gauche conformer is the ground state in the parent polysilane $(SiH_2)_x$.[5] The geometrical structure of *gauche*-polysilane (GP) is quite different from *trans*-polysilane (TP). The electronic structure is expected to be greatly affected by the conformation. We feel that our previous calculations,[3] restricted to only trans conformation, have become insufficient for the present stage of polysilane research.

It is not clear yet whether the thermochromic shift is associated with conformational transition. The theoretical ground is restricted to within MM2 calculations on oligomers. MM2 is not based on quantum mechanics and does not provide any information about electronic structure. Thus, we continue studying the electronic structure of the polysilanes. In the present article, we report the results of more reliable ab initio crystal orbital calculations on the parent polysilane of the various helical structures between trans and gauche conformations.

2. Method of Calculation

We have used the ab initio crystal orbital method with a combined symmetry operation rather than with a simple translation in order to obtain the total energy and the electronic band structure of the parent polysilane. If we take the screw axis coincident with the Cartesian *z* axis, the $\bar{p}_x^j$ and $\bar{p}_y^j$ basis functions belonging to the *j*th cell from the reference cell can be obtained by the rotations of the Cartesian p_x^j and p_y^j orbitals

$$\bar{p}_x^j = p_x^j \cos(j\theta) + p_y^j \sin(j\theta) \quad (1)$$

$$\bar{p}_y^j = -p_x^j \sin(j\theta) + p_y^j \cos(j\theta) \quad (2)$$

where θ is the helical angle of one-dimensional polymers. Performing these rotations on all one- and two-electron integrals, we are able to take *one SiH_2 unit* itself as a *unit cell*. This idea was first implemented by Imamura for the extended Hückel calculations.[6] It was then applied to the CNDO/2 version by Fujita and Imamura[7] and by Morokuma,[8] in succession. The ab initio level calculations were finally reported by Blumen and Merkel.[9] Very recently, this procedure has been applied to more realistic polymer systems.[10] Details of the crystal orbital method have been given in these papers.

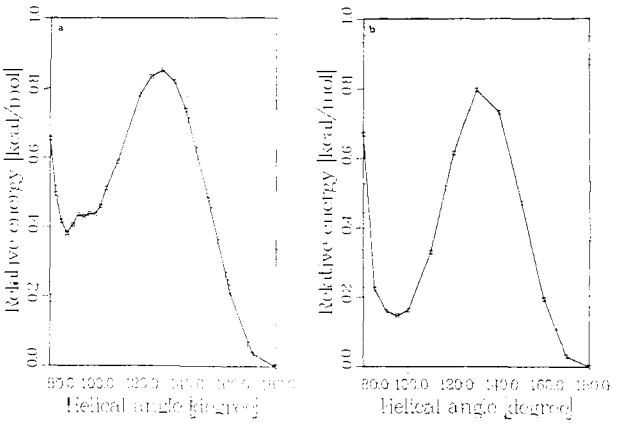

Figure 1. Potential energy surface of polysilane with rotation along the polymer axis between trans and gauche isomers: (a) STO-3G basis set and (b) DZ basis set.

We have used the STO-3G basis set,[11] and further refinements were performed with the Huzinaga–Dunning–Hay double-ζ (DZ) basis set[12] for the polymer calculations. An inclusion of the d-type basis functions for silicon atoms is yet beyond our computational resources. The geometries are optimized for the all-trans conformer. For other conformers, the rigid rotor approximation is employed throughout this study. The optimization is done by the usual crystal orbital method utilizing the translational symmetry only because the energy gradient method for the helical polymers is not yet available.[13] The tenth neighboring SiH_2 interactions are considered in the cellwise summation scheme.[14] Density matrices are obtained with Simpson's rule[15] with the regular interval sampling of 41 *k* points, about half of the Brillouin zone.[16]

(4) (a) Harrah, L. A.; Zeigler, J. M. *J. Polym. Sci., Polym. Lett. Ed.* **1985**, *23*, 209. (b) Miller, R. D.; Hofer, D.; Rabolt, J.; Fickes, G. N. *J. Am. Chem. Soc.* **1985**, *107*, 2172. (c) Rabolt, J.; Hofer, D. Miller, R. D.; Fickes, G. N. *Macromolecules* **1986**, *19*, 611.

(5) (a) Damewood, J. R., Jr.; West, R. *Macromolecules* **1985**, *18*, 159. (b) Tashiro, K.; Unno, M.; Nagase, S.; Teramae, H. *Nippon Kagaku Kaishi* **1986**, 1404. (c) Welsh, W. J.; DeBolt, L.; Mark, J. E. *Macromolecules* **1986**, *19*, 2978.

(6) Imamura, A. *J. Chem. Phys.* **1970**, *52*, 3186.

(7) Fujita, H.; Imamura, A. *J. Chem. Phys.* **1970**, *53*, 4555.

(8) (a) Morokuma, K. *Chem. Phys. Lett.* **1970**, *6*, 186. (b) Morokuma, K. *J. Chem. Phys.* **1971**, *54*, 962.

(9) Blumen, A.; Merkel, C. *Phys. Status Solidi B* **1977**, *83*, 425.

(10) (a) Andrē, J. M.; Vercauteren, D. P.; Bodart, V. P.; Fripiat, J. G. *J. Comput. Chem.* **1984**, *5*, 535. (b) Karpfen, A.; Beyer, A. *J. Comput. Chem.* **1984**, *5*, 11; *J. Comput. Chem.* **1984**, *5*, 19. (c) Otto, P.; Clementi, E.; Ladik, J. *J. Chem. Phys.* **1983**, *78*, 4547.

(11) Hehre, W. J.; Ditchfield, R.; Stewart, R. F.; Pople, J. A. *J. Chem. Phys.* **1970**, *52*, 2769.

(12) (a) Huzinaga, S. *J. Chem. Phys.* **1965**, *42*, 1293. (b) Dunning, T. H.; Hay, P. J. *Modern Theoretical Chemistry*; Schaefer, H. F., Ed.; Plenum: New York, 1977; Vol. 3, pp i–27.

(13) Teramae, H.; Yamabe, T.; Imamura, A. *J. Chem. Phys.* **1984**, *81*, 3564.

(14) The influence of the cutoff scheme on the total energy was discussed in: Teramae, H. *J. Chem. Phys.* **1986**, *85*, 990, and references cited therein.

(15) Davis, P. J.; Rabinowitz, P. *Method of Numerical Integration*; Academic Press: New York, 1975; p 45.

(16) Karpfen recommended $(4n + 1)k$ points sampling for the case of *n*th neighbor interaction calculation: Karpfen, A. *Int. J. Quantum Chem.* **1981**, *19*, 1207.

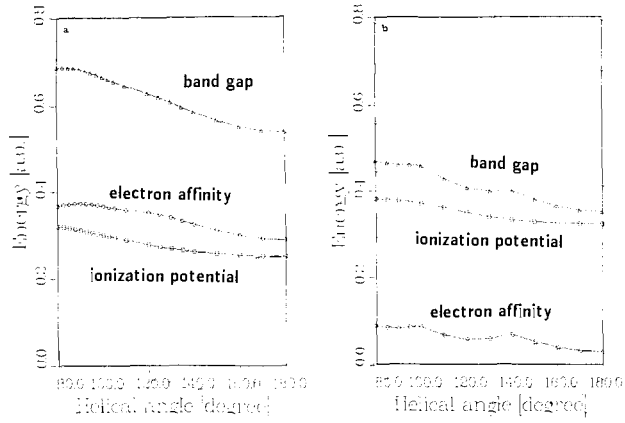

Figure 2. Koopmans' ionization potential, vertical electron affinity, and band gap of polysilane with respect to the helical angle θ: (a) STO-3G basis set and (b) DZ basis set.

The density of states is numerically determined by Brust's histogram method.[17] The effective mass of the hole at the valence band edge and that of the electron at the conduction band edge are calculated with

$$m^* = \hbar^2/(\mathrm{d}^2\epsilon(\mathbf{k})/\mathrm{d}\mathbf{k}^2) \qquad (3)$$

where $\mathrm{d}^2\epsilon(\mathbf{k})/\mathrm{d}\mathbf{k}^2$ is numerically determined by the least-squares fits of the calculated energy band structures.[18] The effective mass is an important index for the semiconductive and metallic materials because an electron carrier reacts as a particle of mass m^* in the external electric field.

3. Results and Discussion

Table I lists the optimized structures of TP and *all-trans*-Si_nH_{2n+2} clusters (n = 3–5) for a comparison.[19] The values are consistent with previous band calculations at the ab initio ECP level,[3a] although the previous calculations employed some important approximations (insufficient lattice summations, symmetric cutoff, and projecting out of basis functions)[20] so direct comparison should be avoided. The total energy of cluster calculations converged well and are almost identical with the band calculations even for pentasilane (n = 5). Note that the STO-3G basis set gives a shorter Si–Si bond length.

Figure 1 shows the energy difference with respect to the helical angle θ.[21] TP is more stable than GP by 0.38 kcal/mol per SiH_2 unit, using the STO-3G basis set. Further optimization of the GP structure results in an energy lowering of 0.000 02 au (0.02 kcal/mol), which has no effect on this conclusion. The energy difference becomes smaller (0.15 kcal/mol per SiH_2 unit) with the DZ basis set. The GP helical angles are near the perfect 90°, i.e., 87.5° at the STO-3G level and 95° at the DZ level. The extra energy minimum around 100° in the STO-3G results is caused by neglect of the geometry optimization with respect to every helical angle. The same result was reported for the polyethylene calculation. This energy minimum was found to disappear, relaxing all the geometrical parameters.[10b] In the DZ level, there is no such minimum on the potential energy surface. The energy minimums are, therefore, only TP and GP in the parent polysilane.

Figure 2 shows Koopmans' ionization potential, vertical electron affinity, and band gap with respect to the helical angle θ. All values increase as θ decreases, producing larger values for GP than TP. The band gap difference could be a cause of the thermochromic shift. The calculated band gap difference, 2.96 eV, is far from that observed in the experiment. Electron acceptor doping is more effective in TP due to the small TP ionization potential. The conformational dependence of the ionization potential and the band gap discussed above are consistent with the previous semiempirical CNDO/INDO cluster calculations.[22]

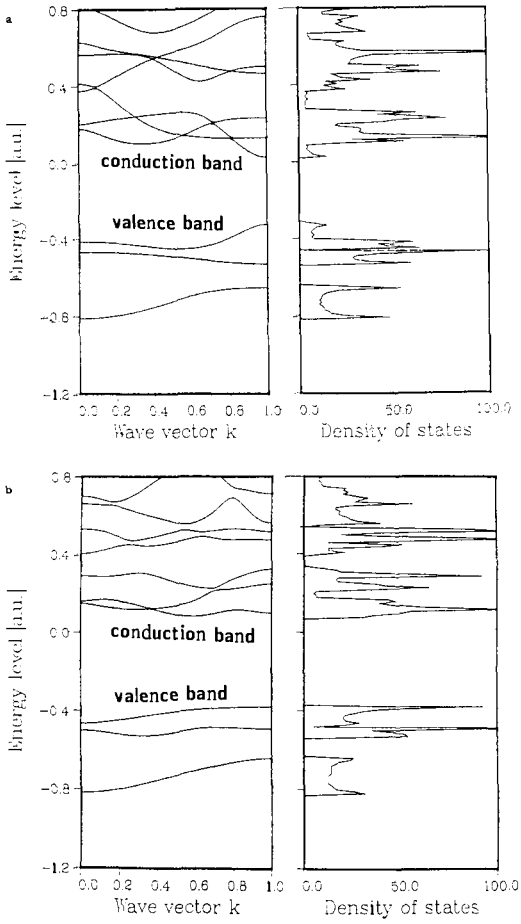

Figure 3. Double-ζ energy band structures of (a) *trans*- and (b) *gauche*-polysilanes.

Table II. Effective Masses of the Hole at the Valence Band Edge and Koopmans' Ionization Potentials of *trans*-Polysilane, *gauche*-Polysilane, *trans*-Polyethylene, and *trans*-Polyacetylene (All Calculations at STO-3G Levels)

compd	effective mass[a]	ionization potential[b]
trans-polysilane	0.14	6.8
gauche-polysilane	20.91	8.5
trans-polyethylene[c]	0.21	9.9
trans-polyacetylene[d]	0.12	5.2

[a] Units are in mass of a free electron. [b] Units are in electronvolts. [c] The geometry is taken from Karpfen's work.[10b] [d] The geometry is taken from our previous work.[14]

Figure 3 shows the DZ energy band structure of TP and GP. The STO-3G energy band structure is very similar to these and is omitted here. TP has a direct-absorption-type band gap, while GP has an indirect-absorption-type band gap. The conduction band edge of GP is not at the Brillouin zone boundary.[23] GP, therefore, would have little photoluminescence, because nonradiative recombination of the hole-electron pair usually occurs in indirect-type materials such as solid silicon. This indirect-ab-

(17) Brust, D. *Methods in Computational Physics*; Alder, B., Fernbac, S.; Rotenberg, M., Eds.; Academic Press: New York, 1968; Vol. 8, p 33.
(18) See, for example: Kittel, C. *Introduction to Solid State Physics*, 5th ed.; Wiley: New York, 1976; pp 218–219.
(19) Cluster calculations are performed with the GAUSSIAN82 program package: Binkley, J. S.; Frisch, M. J.; DeFrees, D. J.; Krishnan, R.; Whiteside, R. A.; Schlegel, H. B.; Fluder, E. M.; Pople, J. A. *GAUSSIAN82*; Carnegie-Mellon University: Pittsburgh, PA, 1983.
(20) Karpfen, A., private communication, 1983.
(21) Reference 8b showed the relation between the helical angle θ and the Si–Si–Si–Si distortion angle. The latter is more commonly used to specify molecular structures and is particularly widely used in quantum chemistry programs such as MM2 or GAUSSIAN82.
(22) (a) Bock, H.; Ensslin, W.; Fehér, F.; Freund, R. *J. Am. Chem. Soc.* **1976**, *98*, 668. (b) Kligensmith, K. A.; Downing, J. W.; Miller, R. D.; Michl, J. *J. Am. Chem. Soc.* **1986**, *108*, 7438.
(23) Of course, the conduction bands are not optimized at the present Hartree–Fock level, and the properties about the conduction band should be treated with caution. In the present case, we confirm that the STO-3G band structure gives the same result. The present conclusion may be changed by more accurate calculations.

Table III. Classification of σ-Framework Polymers

class	ionization potential	effective hole mass	predicted characteristic[a]	example
supra σ-conjugative	small	small	semiconductor	*trans*-polysilane
infra σ-conjugative	large	small	insulator	*trans*-polyethylene
non σ-conjugative	large	large	insulator	*gauche*-polysilane

[a] After doping with an electron accepter.

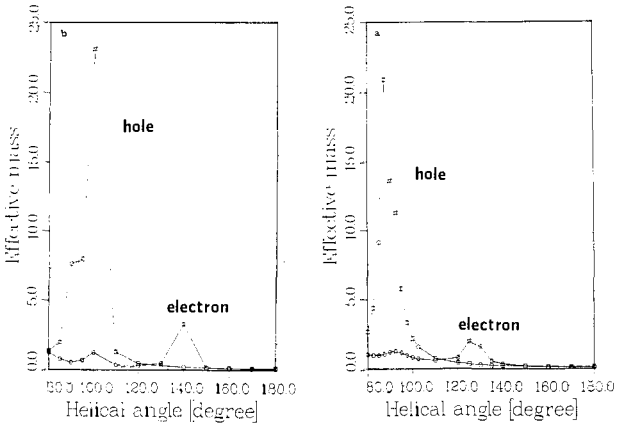

Figure 4. Effective mass of hole at valence band edge and electron at conduction band edge: (a) STO-3G basis set and (b) DZ basis set.

sorption-type band gap is a characteristic feature of polysilanes. The carbon analogue polyethylene in its imaginary gauche form has the direct-absorption-type band gap.

In TP, the highest valence band has rather larger dispersion in the vicinity of the Brillouin zone boundary.[24] On the other hand, in GP, there is little dispersion in the vicinity of the valence band edge. The electrons are, therefore, delocalized in TP and localized in GP. The localization of electrons is clearly seen from the density of states, also shown in Figure 3. The density of state of GP has a sharper peak at the valence band edge than that of TP.

To confirm this situation more quantitatively, we calculate the effective masses of the hole at the valence band edge m_h^* and the electron at the conduction band edge m_e^* that are shown in Figure 4. The value of m_h^* greatly depends on the helical angle θ, whereas that of m_e^* does not. The GP m_h^* by DZ is $7.99m_0$, being 66 times heavier than the TP m_h^*, $0.12m_0$. The GP m_h^* by STO-3G is $20.90m_0$, being 149 times heavier than the TP m_h^*, $0.14m_0$, where m_0 is the mass of a free electron. This means that the hole conductivity along the silicon backbone is expected to be much larger in TP.

The problem is now why the m_h^* of TP is so light or why the TP electrons are so delocalized. The valece band edge of the polysilane (both TP and GP) consists of one of the singly occupied molecular orbitals of the H_2Si: radical. This is the pure 3p orbtial of the silicon atom as shown in Figure 5. The orbital interaction is maximum at the all-trans conformation because the orbital stands in a coplane. On the other hand, the orbital is not coplanar, and the orbital interaction becomes smaller in the all-gauche conformation, as shown in Figure 5. The theory of orbital interaction tells us that the larger the orbital interaction becomes, the wider the energy levels separate. The effective mass decreases by definition (eq 3) when the energy levels separate. In other words, the resonance integrals between two Si–Si σ-bonds become the largest and the degree of σ-delocalization is maximum at the trans conformation.

Table II summarizes the effective hole mass and the ionization of TP, GP, *trans*-polyethylene (PE), and *trans*-polyacetylene (PA) at the STO-3G level.[25] The effective masses of TP and PA are

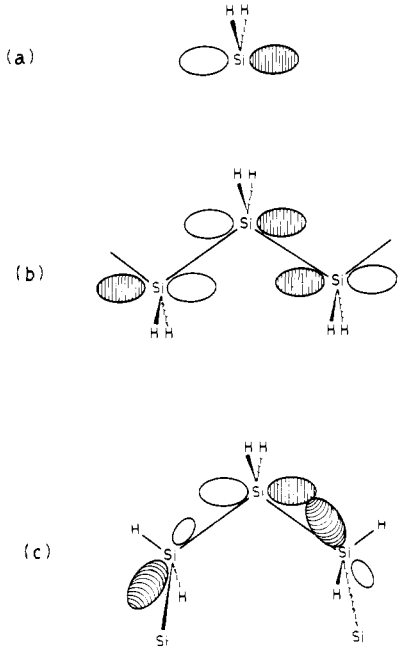

Figure 5. Schematic representation of orbitals: (a) the highest singly occupied orbital of SiH_2, (b) orbital corresponding to the valence band edge of *trans*-polysilane, and (c) orbital corresponding to the valence band edge of *gauche*-polysilane.

comparable. It is surprising that the effective mass of PE is only $0.21m_0$, suggesting that PE may conduct electricity if there are sufficient carriers (holes). This fact agrees well with the conclusion from a photoconduction experiment.[26] Unfortunately, the ionization potential of PE is so large that no dopants can create sufficient holes. This is why PE remains an insulator. In PE, the σ-conjunction exists but it is not significant. GP has a high ionization potential and large effective mass, so it is also expected to be an insulator. Therefore, the σ-framework polymers should be classified into three types as shown in Table III, apart from the π-type polymers.[27] The supra σ-conjugative class is the most important for research on synthetic metals. TP belongs to this class. Recently, Nelson and Pietro also discussed the σ-conjugation in polysilane.[28] They concluded that the σ-conjugation was attributed to the relatively high energy and highly diffuse nature of the Si–Si σ-bond. This conclusion is not sufficient as discussed above. From their conclusion the difference between trans and gauche structures is never explained.

4. Conclusions

Our studies of the electronic structure of the parent polysilanes with trans and gauche conformations employing the ab initio Hartree–Fock crystal orbital method with standard STO-3G and DZ basis sets yield the following conclusions:

(1) Both TP and GP are the minimum on the potential energy surface of the parent polysilanes. TP is calculated to be more stable than GP by 0.38 kcal/mol per SiH_2 unit at the STO-3G level and 0.15 kcal/mol per SiH_2 unit at the DZ level.

(2) GP has a larger ionization potential and band gap than TP.

(24) The highest valence band and the lowest conduction band correspond to HOMO and LUMO of the molecular case.

(25) The absolute values of the ionization potential are not completely accurate and are underestimated because the minimal STO-3G basis set is used.

(26) Less, K. J.; Wilson, E. G. *J. Phys. C* **1973**, *6*, 3110.

(27) Since the ionization potential is always small enough whenever the π-conjugation exists, such a classification is trivial for the π-type polymers.

(28) Nelson, J. T.; Pietro, W. J. *J. Am. Chem. Soc.* **1988**, *92*, 1365.

(3) Since the effective mass of the hole at the valence band edge is extremely small in TP compared to GP, the σ-conjugation is larger in TP. The conservation of the near trans conformation is important if the polysilanes are to be good semiconductors.

(4) The combination of a small effective hole mass and ionzation potential is an important condition in the design of a new conducting material.

Acknowledgment. It is our great pleasure to have discussed polysilanes with Dr. Nobuo Matsumoto and Dr. Masaie Fujino. Informal discussions with Hiroshi Kojima and Hiroaki Isaka were relaxing and supportative. We thank Dr. Takunori Mashiko for instruction in the use of the graphic program library.

Registry No. GP,TP, 32028-95-8.

Synthesis of Dialkyl- and Alkylacylrhenium Complexes by Alkylation of Anionic Rhenium Complexes at the Metal Center. Mechanism of a Double Carbonylation Reaction That Proceeds via the Formation of Free Methyl Radicals in Solution

Karen I. Goldberg and Robert G. Bergman*

Contribution from the Department of Chemistry, University of California at Berkeley, Berkeley, California 94720. *Received June 6, 1988*

Abstract: The site of alkylation of salts of acylrhenates such as $Li^+[Cp(CO)_2Re(COCH_3)]^-$ (**1**) can be controlled by adjusting the hardness of the alkylating agent. Thus, treatment of **1** with the hard alkylating agent $(CH_3)_3OPF_6$ gives predominantly the classical Fischer carbene complex $Cp(CO)_2Re{=}C(OCH_3)(CH_3)$ (**2**), whereas reaction with the softer electrophile CH_3I leads almost exclusively to the new metal-alkylated complex $Cp(CO)_2Re(CH_3)(COCH_3)$ (**3**). The structure of **3** has been determined by X-ray diffraction. The availability of this material, a relatively rare example of a stable alkylacylmetal complex, has provided an opportunity to study the products and mechanisms of its carbon–carbon bond-forming decomposition reactions. Thermally, the alkyl acyl complex undergoes simple reductive elimination, leading (in the presence of a metal-scavenging ligand L) to a quantitative yield of acetone and $CpRe(CO)_2(L)$. Photochemically, a more complicated reaction takes place, especially under 20 atm of CO, where $CpRe(CO)_3$ and 2,3-butanedione are formed. Strikingly, irradiation of $Cp(CO)_2Re(CH_3)_2$ (**9**) under 20 atm of CO gives products identical with those formed from **3**. Labeling experiments using ^{13}CO and mixtures of acetyl- and propionylrhenium complexes are inconsistent with a mechanism involving simple migratory CO insertion followed by reductive elimination. They are, however, consistent with metal–carbon bond homolysis leading to methyl and acetyl radicals, followed by carbonylation of the methyl radicals to give a second source of acetyl radicals; these reactive intermediates then dimerize to give 2,3-butanedione. Confirmation of this mechanism was obtained by trapping all the initially formed radicals with halogen donors. $BrCCl_3$ proved to be much more efficient than CCl_4 for this purpose: irradiation of alkyl acyl complex **3** in the presence of $BrCCl_3$ diverted the reaction completely from 2,3-butanedione production, giving instead CH_3Br, CH_3COBr, $Cp(CO)_2Re(CH_3)Br$, and $Cp(CO)_2Re(CH_3CO)Br$.

Elimination of ketones from acyl alkyl transition-metal complexes, as depicted in Scheme I, occurs rapidly compared to the similar reductive coupling of two alkyl ligands to form alkanes.[1a] The facility of this elimination reaction has hindered the isolation, characterization, and study of acyl alkyl complexes.[2]

In view of this high reactivity, acyl alkyl species have often been invoked as undetected intermediates in ketone-forming reactions. The reaction of Collman's reagent, $Na_2Fe(CO)_4$, with alkyl halides to yield ketones is postulated to proceed through such an acyl alkyl intermediate.[3] A mononuclear acetyl methyl derivative has been suggested as an intermediate in the decomposition of $[CpCo(CO)CH_3]_2$ and in the reaction of CO with $CpCo(CH_3)_2PPh_3$ to give acetone.[4] The reaction of Cp_2TiR_2 (R = Ph) with CO at room temperature[5] and the carbonylation reactions of NiR_2L_2 (R = Me, Et) to give RCOR[6] are presumed to go through analogous intermediates. Reductive elimination of ketone from diacyl anionic derivatives of rhenium and manganese carbonyl complexes was shown to be preceded by CO deinsertion forming acyl alkyl complexes.[2] However, only in the rhenium system were such acyl alkyl complexes isolable.

Scheme I

Scheme II

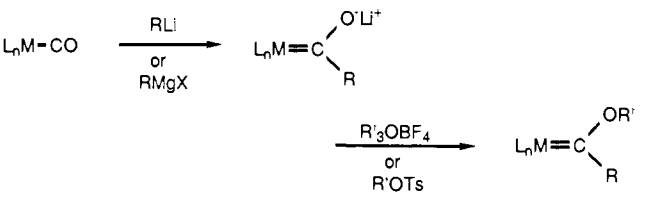

The research described in this paper was stimulated by the discovery of a potentially general procedure for preparing acy-

(1) Collman, J. P.; Hegedus, L. S.; Norton, J. R.; Finke, R. G. *Principles and Applications of Organotransition Metal Chemistry*, 2nd ed.; University Science Books: Mill Valley, CA, 1987; references cited therein, (a) Chapter 5, (b) p 107, (c) p 244, (d) p 764.

(2) Casey, C. P.; Scheck, D. M. *J. Am. Chem. Soc.* **1980**, *102*, 2723, and references therein.

(3) Collman, J. P. *Acc. Chem. Res.* **1975**, *8*, 342.

(4) (a) Schore, N. E.; Ilenda, C. S.; White, M. A.; Bryndza, H. E.; Matturo, M. G.; Bergman, R. G. *J. Am. Chem. Soc.* **1984**, *106*, 7451. (b) Evitt, E. R.; Bergman, R. G. *J. Am. Chem. Soc.* **1980**, *102*, 7003.

(5) Masai, H.; Sonogashira, K.; Hagihara, N. *Bull. Chem. Soc. Jpn.* **1968**, *41*, 750.

(6) Yamamoto, T.; Kohara, T.; Yamamoto, A. *Bull. Chem. Soc. Jpn.* **1981**, *54*, 2161.

0002-7863/89/1511-1285$01.50/0